Study of diacetyl-water clusters using Raman scattering and quantum-chemical method

A. Jumabaev, H. Hushvaktov, A. Absanov, A. Norkulov*, B. Iltizarov

Samarkand State University, University blv. 15, 140104, Samarkand, Uzbekistan

Received 07.06.2022, revised 21.06.2022

* Corresponding author: e-mail norqulovasliddin1987@gmail.com, Phone: +998 93 851 52 87

В настоящей работе межмолекулярные взаимодействия диацетила и молекул воды изучены с использованием колебательного спектра. Проанализированы спектры комбинационного рассеяния, полученные в диапазоне 500–2000 см$^{-1}$, и сопоставлены с результатами. Также впервые были изучены распределения плотности заряда и 3D графики потенциальной энергии с использованием модели симуляции для молекул диацетила. С увеличением числа молекул при образовании молекулярных кластеров с молекулой воды наблюдается насыщение энергии межмолекулярного взаимодействия, соответствующей одиночной H-связи. Это соответствует молекулярным кластерам DA+$(H_2O)_3$ и позволяет сделать вывод о стабильности этого кластера по отношению к другим.

Ключевые слова: диацетил, вода, DFT расчеты, комбинационные спектры рассеяния, водородная связь.

In this work, the intermolecular interactions of diacetyl and water molecules were studied using the vibration spectrum. The Raman scattering spectra obtained in the range of 500–2000 cm^{-1} were analyzed and compared with the results of calculations. For the first time also, the charge density distribution and 3D potential energy graphs are examined using simulations for diacetyl molecules. With the increase in the number of molecules at the formation of molecular clusters with the water molecule, the saturation of the intermolecular interaction energy corresponding to a single H-bond is observed. This corresponds to DA+$(H_2O)_3$ molecular clusters and allows one to conclude that this cluster is stable relative to the others.

Keywords: diacetyl, water, DFT calculations, Raman scattering spectrum, hydrogen bonding.

DOI: https//doi.org/10.52304/.v24i2 329

I. Introduction

Now, it has been established that noncovalent interactions, in particular hydrogen bonding, play an important role in atmospheric chemistry, astrophysics, as well as many biochemical and catalytic processes [1-3]. 1,2-butadione or biacetyl are other names for diacetyl (DA) [4-8]. Dargent et al [1] studied two different S1 and S2 isomers of the diacetyl-water system by FTIR spectroscopy in a neon matrix and by anharmonic ab-initio calculations, and determined that the O-H stretching vibration was the most stable for the diacetyl-water system. Because, it causes an increase in the amount of carbosol in the atmosphere, DA in the gaseous phase has been studied in the far and near IR regions (25–600 cm^{-1} and 520–6500 cm^{-1}) [5]. Kamei et al. [9] have used the fluorescence method to study the transitions in DA atoms and observed the presence of extra overtones in addition to the main vibration bands. Johnson and Holman [10] studied the properties of DA by mass-spectroscopy. Using Fure spectroscopy and theoretical calculations, Favero and Caminati [11] studied the connection of three different conformations of DA with water molecules and discovered that DA forms strong O···H-O and weak O···H-C hydrogen bonds with water.

The rotational spectrum of the molecular complex DA-water has been measured by pulsed jet

Fourier transform microwave (FTMW) spectroscopy. The water molecule acts as an electrofore and induces a dipole moment when combined with nonpolar diacetyl. Only one conformer has been observed, corresponding to the global minimum [11]. Since diacetyl is used in many foods (wine production, e-cigarettes, etc.) and also has harmful effects for human health [12-17]. It is important to study the interaction of diacetyl with water in the human body, especially as it can cause lung cancer. The above considerations require further research in diacetyl and its aqueous solutions. It is clear from the literature cited above that there are still unresolved issues regarding the manifestation of DA and its aqueous solutions in the vibration spectrum. Therefore, in this work, an attempt has been made to explain the manifestation of DA and its aqueous solutions in the spectra of Raman scattering through experimental and theoretical calculations.

II. Experimental and calculation methods

The Raman spectrum was obtained with an InViaRaman spectrometer. A Stabilized Laser Module with a power of 100 mW and a wavelength of 785 nm and a diffraction grating with a constant of 1200 line/mm were used as the excitation light source. The spectra were recorded using a Renishaw CCD camera detector.

The laser beam was focussed on the surface of the samples to a diameter of 10 microns for the measurements. For radiation of the sample surface was used the direct magnified objective excitation light, which varied depending on the size of the output signal on the detector, as well as to collect scattered light. The recording time was 10 s., and the measurements were made in extended mode, which allows measurements to be made in the desired wavelength range.

Quantum-chemical calculations were performed based on the Gaussian 09 program B3LYP/DFT (density function theory) method and bases set 6-311++G (d,p) for isolated diacetyl and water molecule monomers, diacetyl dimer aggregates and diacetyl-water clusters [18].

III. Results and discussions

Figure 1 shows the Raman scattering spectra of DA obtained in the region of 500–2000 cm^{-1}. As can be seen from Fig. 1a, the Raman scattering spectra of pure DA are complex and consist of several bands with different depolarization ratios. There is the skeletal band (vibration) corresponds to a 697 cm^{-1} band which has asymmetry on the high frequency side. In the theoretical calculation (Fig. 1b), 683 cm^{-1} line corresponds to this band (Table 1) and the difference between the wave numbers is 13 cm^{-1}. The 1011 cm^{-1} band, on the other hand, corresponds to the C-C stretching vibration and appears as the sum of two bands with low intensity.

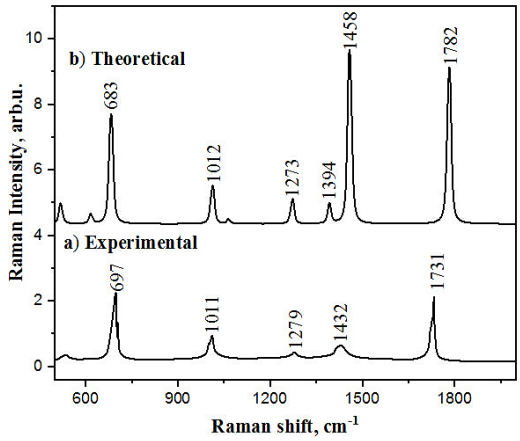


Figure 1. Raman spectra of pure DA obtained in the range of 500–2000 cm^{-1}: a) experimental, b) theoretical.

Table 1. Experimental and theoretical selected frequencies of DA.

Mode No.	Observed frequency (cm^{-1})	Calculated frequencys (cm^{-1})		Assignment
(i)	Raman	Calculated	Obs./Calc.	
1	697	683	1.02	Skeletal bend
2	1011	1012	0.99	C-C stretching
3	1279	1273	1.004	CH_3-rock
4		1394		Symmetric CH_3-bend
5	1432	1458	0.98	Asymmetric CH_3-bend
6	1731	1782	0.97	C=O stretching

©Academy of Sciences of Republic of Uzbekistan, 2022

In theoretical calculation, this band is corresponded to 1012 cm^{-1}. The CH_3-bending vibration corresponds to 1279 cm^{-1} band, which theoretically corresponds to 1273 cm^{-1} and difference between observed and calculation bands is 6 cm^{-1}. The asymmetric CH_3-bending vibration corresponds to band of 1432 cm^{-1}, the spectral band has a slightly larger half-width, and in theoretical calculation this band is 1458 cm^{-1} (differs by 26 cm^{-1}).

There are two C=O vibration in the DA molecule. It is interesting to learn represented in the vibration spectra these stretching vibration bands. In the experiment, C=O stretching vibration corresponds to 1731 cm^{-1} and has asymmetry on the low frequency side. Compared with the result found by the theoretical calculations, 51 cm^{-1} shift towards a higher frequency side and the two bands 1782 cm^{-1} and 1783 cm^{-1} corresponding to the C=O stretching vibration can be seen. This indicates the complexity of the spectral bands and may be related to the overlap of the spectral lines belonging to different associations [19]. According to the results of Raman scattering spectra obtained in the region of 500–2000 cm^{-1}, the experimental and theoretical calculations differ from each other by ±2%.

Calculations were performed for DA and water monomer, DA dimer and complexes of DA with water molecules. Figures 2a and 2c show DA and water monomers. DA monomers (O12); (N10) and (O11); (N3) atoms are located in opposite planes to each other, and the distances between the atoms are the same 2.55 Å. This leads to the conclusion that there is a possibility of a weak intermolecular hydrogen bond in the DA monomer molecule, and that this intermolecular hydrogen bond is also maintained in the DA dimer.

The charge distributions for DA monomer, dimer, and water-formed aggregates are given in Table 3. The table shows that the C1, C7, O11 and O12 atoms in the DA monomer are negatively charged, while the remaining atoms are positively charged. Due to the redistribution of charges in the formation of aggregates, the amount of charge in the atoms changes, and this change is greater in the atoms involved in the H-bond. In the DA dimer, the H8 and O11 atoms are involved in the H-hydrogen bond, and their charges changed from 0.181 to 0.224 and from -0.252 to -0.233, respectively.

In Fig. 2b the DA dimer is shown. As can be seen from the figure, the closed structural aggregates of different types: O11...H16-2.474 Å and O24...H8-2.474 Å are formed by hydrogen bonds (atomic number is shown in the figure and Table 2). The energy of dimer formation is E=1.58 kcal/mol and the dipole moment is 0.001 D. The charge of the two oxygen atoms involved in the H-bond decreased by the same –0.230 (–0.249 in the monomer) and the charge of the hydrogen atom increased by +0.218 (+0.177 in the monomer). The Raman spectra obtained in ab-initio calculations for the monomeric and dimeric aggregates of the DA molecule are given (Fig. 3). In the calculations, two bands 1782 and 1783 cm^{-1} correspond to the C=O stretching vibration of the DA monomer molecule (depolarization ratios 0.50 and 0.00), and in the dimer 1776 cm^{-1}, 1777 cm^{-1}, 1780 cm^{-1} and 1781 cm^{-1} bands (depolarization ratios 0.47, 0.42, 0.74, and 0.47, respectively) form a bond with a single H atom in the CH_3 group.

DA is the simplest representative of biologically active substances and the interactions and orientations of 5 water molecules with DA were studied because it was interesting to observe the formation of molecular clusters with the water molecule and its manifestation in the vibration spectra.

Figure 2d shows clusters DA+$(H_2O)_1$. As can be seen from the figure, H-bond is formed between the O11 atom of DA and the H14 atom of the water molecule with bond length being 1.973Å. The energy of formation of such a cluster is E=3.28 kcal/mol (Table 2). The Raman spectra obtained in the theoretical calculations for the DA+$(H_2O)_1$ clusters are shown in Fig. 4. As can be seen from the figure, the bands 1771 cm^{-1} and 1780 cm^{-1} correspond to the C=O stretching vibration cluster DA+$(H_2O)_1$.

Figure 2e shows clusters of DA+$(H_2O)_2$, where two oxygen atoms in the C=O group of DA are also involved in H-bonding. The length of the H-bond are are O8...H12-1.975 Å, O11...H17-1.986 Å and equal each other. The energy of cluster formation is E = 6.54 kcal/mol (Table 2). Theoretical calculations show that in the DA+$(H_2O)_2$ cluster, the bands 1750 cm^{-1} and 1775 cm^{-1} correspond to the C=O stretching vibration in the Raman spectra.

A similar feature was observed in cluster DA+$(H_2O)_3$ (Fig. 2f) and in cluster DA+$(H_2O)_2$ (Fig. 2e). The two oxygen atoms in the C=O group are involved in the formation of the H-bond. The bond lengths are for O12...H17- 1.997 Å,

©Academy of Sciences of Republic of Uzbekistan, 2022

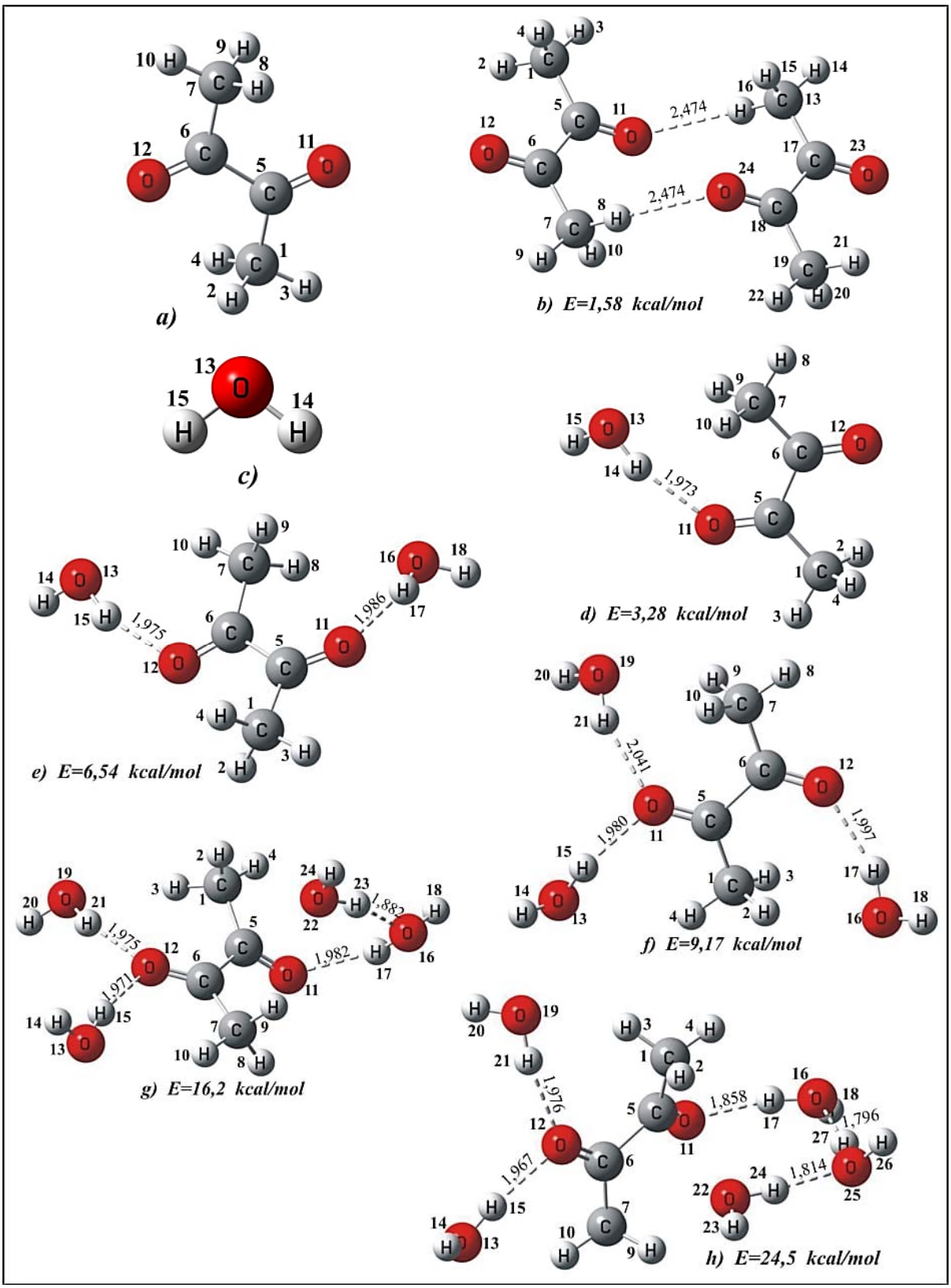


Figure 2. The structure of diacetyl and water clusters: a) monomer, b) dimer, c) water monomer,d) DA+$(H_2O)_1$,e) DA+$(H_2O)_2$, f) DA+$(H_2O)_3$, g) DA+$(H_2O)_4$,h) DA+$(H_2O)_5$. Here: red - oxygen, gray - carbon and white – hydrogen.

©Academy of Sciences of Republic of Uzbekistan, 2022

Table 2. Results of ab-initio calculations for diacetyl molecule.

Structure	Bond length, (Å)	Frequency C=O, cm^{-1} (Raman activity, A^4/AMU)	Polarization ratio (ρ)C=O	Dipole moment, (D)	Energy of complex formation kcal/mol
DA monomer		1782(32,70) 1783 (0)	0.50 0.00	0	
DA dimer	r(O^{24}…H^{8})=2,474 r(O^{11}…H^{16})=2,474	1776 (00.00) 1777 (78.47) 1780(0) 1781 (11.21)	0.47 0.42 0.74 0.47	0.001005	1.58
DA + $(H_2O)_1$	r(O^{11}…H^{14})=1.973	1771 (18.64) 1780 (21.12)	0.39 0.41	2.029997	3.28
DA + $(H_2O)_2$	r(O^{11}…H^{17})=1.986 r(O^{12}…H^{15})=1.975	1771 (15.61) 1775 (27.06)	0.29 0.34	3.597432	6.54
DA + $(H_2O)_3$	r(O^{11}…H^{15})=1.980 r(O^{12}…H^{17})=1.997 r(O^{11}…H^{21})=2.041	1750 (20.59) 1773 (34.25)	0.24 0.31	1.866252	9.17
DA + $(H_2O)_4$	r(O^{12}…H^{15})=1.971 r(O^{12}…H^{21})= 1.975 r(O^{11}…H^{17})=1.982 r(O^{16}…H^{23})=1.882	1747 (15.56) 1766 (31.87)	0.26 0.27	2.947551	16.2
DA + $(H_2O)_5$	r(O^{12}…H^{21})=1.976 r(O^{12}…H^{15})=1.967 r(O^{11}…H^{17})=1.858 r(O^{16}…H^{27})=1.796 r(O^{25}…H^{24})=1.814	1748 (9.04) 1761 (39.51)	0.26 0.23	2.199827	24.5

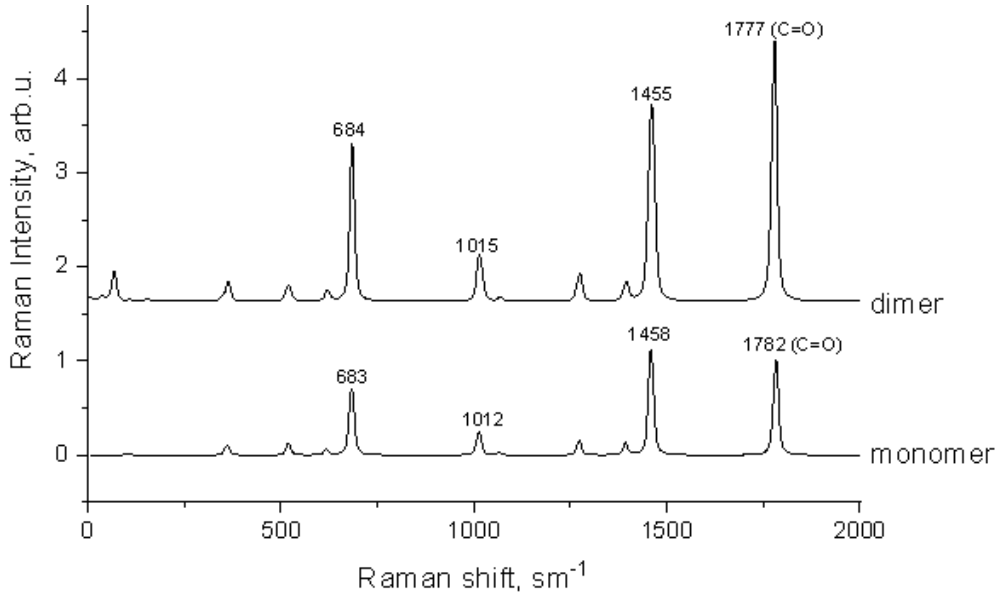


Figure 3. Calculated Raman spectra of DA monomer and dimer aggregates.

©Academy of Sciences of Republic of Uzbekistan, 2022

Table 3. Charge distribution in DA water clusters.

DA Monomer		DA dimer		DA+$(H_2O)_1$		DA+$(H_2O)_2$		DA+$(H_2O)_3$		DA+$(H_2O)_4$		DA+$(H_2O)_5$	
Atom number	Charge	Atom number	Charge	Atom number	Charge	Atom number	Charge	Atom number	Charge	Atom number	Charge	Atom number	Charge
C^1	-0.53	C^1	-0.56	C^1	-0.60	C^1	-0.60	C^1	-0.62	C^1	-0.63	C_1	-0.59
H^2	0.18	H^2	0.19	H^2	0.19	H^2	0.19	H^2	0.23	H^2	0.21	H_2	0.22
H^3	0.17	H^3	0.17	H^3	0.17	H^3	0.18	H^3	0.20	H^3	0.22	H_3	0.21
H^4	0.18	H^4	0.18	H^4	0.18	H^4	0.18	H^4	0.18	H^4	0.17	H_4	0.16
C^5	0.26	C^5	0.31	C^5	0.29	C^5	0.14	C^5	0.41	C^5	0.10	C_5	0.09
C^6	0.26	C^6	0.19	C^6	0.26	C^6	0.36	C^6	0.17	C^6	0.54	C^6	0.43
C^7	-0.53	C^7	-0.57	C^7	-0.57	C^7	-0.57	C^7	-0.67	C^7	-0.66	C^7	-0.62
H^8	0.18	H^8	0.22	H^8	0.18	H^8	0.22	H^8	0.18	H^8	0.19	H^8	0.18
H^9	0.18	H^9	0.18	H^9	0.22	H^9	0.19	H^9	0.24	H^9	0.21	H^9	0.21
H^{10}	0.18	H^{10}	0.17	H^{10}	0.18	H^{10}	0.19	H^{10}	0.19	H^{10}	0.20	H^{10}	0.19
O^{11}	-0.25	O^{11}	-0.23	O^{11}	-0.26	O^{11}	-0.24	O^{11}	-0.28	O^{11}	-0.24	O^{11}	-0.22
O^{12}	-0.25	O^{12}	-0.24	O^{12}	-0.24	O^{12}	-0.23	O^{12}	-0.24	O^{12}	-0.30	O^{12}	-0.29
		C^{13}	-0.57	O^{13}	-0.54	O^{13}	-0.52	O^{13}	-0.52	O^{13}	-0.53	O^{13}	-0.52
		H^{14}	0.18	H^{14}	0.29	H^{14}	0.25	H^{14}	0.25	H^{14}	0.25	H^{14}	0.25
		H^{15}	0.17	H^{15}	0.26	H^{15}	0.27	H^{15}	0.26	H^{15}	0.27	H^{15}	0.27
		H^{16}	0.22			O^{16}	-0.54	O^{16}	-0.54	O^{16}	-0.55	O^{16}	-0.57
		C^{17}	0.19			H^{17}	0.29	H^{17}	0.28	H^{17}	0.29	H^{17}	0.31
		C^{18}	0.31			H^{18}	0.26	H^{18}	0.27	H^{18}	0.27	H^{18}	0.27
		C^{19}	-0.56					O^{19}	-0.52	O^{19}	-0.54	O^{19}	-0.54
		H^{20}	0.18					H^{20}	0.27	H^{20}	0.26	H^{20}	0.26
		H^{21}	0.19					H^{21}	0.27	H^{21}	0.29	H^{21}	0.29
		H^{22}	0.17							O^{22}	-0.64	O^{22}	-0.66
		O^{23}	-0.24							H^{23}	0.34	H^{23}	0.29
		O^{24}	-0.23							H^{24}	0.30	H^{24}	0.38
												O^{25}	-0.60
												H^{26}	0.26
												H^{27}	0.34

O11...H15-H15-1.980 Å and O11...H21-2.041 Å. The energy of cluster formation is to *E*=9.17 kcal/mol (Table 2). It can be seen, that in DA+$(H_2O)_3$ clusters the band corresponding to the C=O stretching vibration is divided into two (1750 cm^{-1} and 1773 cm^{-1}) (Fig. 4).

When we look at clusters of DA+$(H_2O)_4$ (Fig. 2g), four different types of hydrogen bonds are formed, the bond lengths are 1.971 Å for O12...H15, 1.975 Å for O12...H21, 1.982 Å for O11...H17 and 1.882 Å for O16...H23. Two 1747 and 1766 cm^{-1} bands belonging to the C=O stretching vibration can be observed (Fig. 3). Cluster formation energy *E*=16.2 kcal/mol (Table 2). In the Raman spectra obtained by theoretical calculations, it can be seen that in DA+$(H_2O)_4$ cluster the same cluster appearance was found (Fig. 4). Theoretical calculations show that in the DA+$(H_2O)_4$ cluster, the bands 1747 cm^{-1} and 1766 cm^{-1} correspond to the C=O stretching vibration in the Raman spectra.

In the formation of five clusters of DA+$(H_2O)_5$ different types of hydrogen bond with bond lengths are (O12...H21-1.976 Å; O12...H15-1.967 Å; O11...H17-1.858 Å; O16...H27-1.796 Å and O25...H24-1.814 Å. By observing the bands 1748 cm^{-1} and 1761 cm^{-1}, which belong to the C=O stretching vibration, we can see that the monomer band shifts towards a lower frequency side. The energy of cluster formation is *E*=24.5 kcal/mol (Table 2).

©Academy of Sciences of Republic of Uzbekistan, 2022

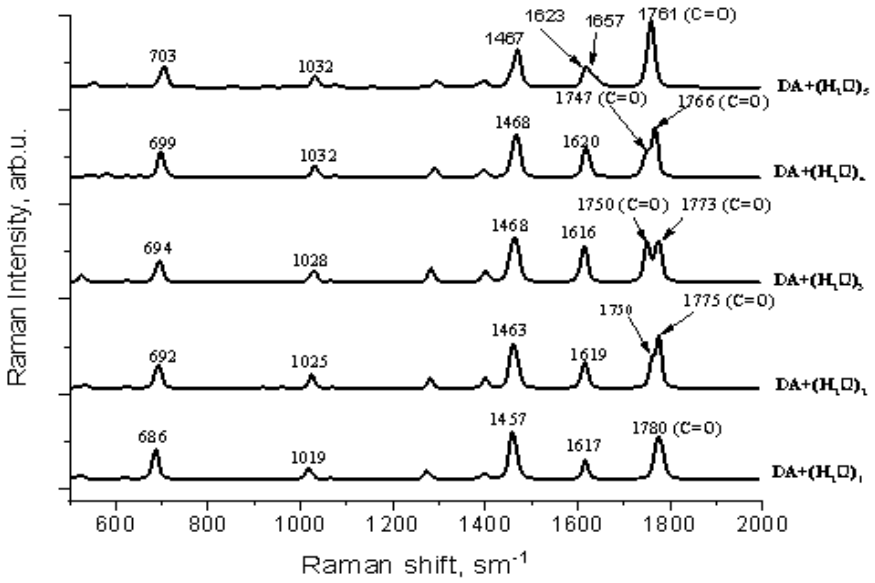


Figure 4. Calculated Raman spectra of DA-water dimer clusters.

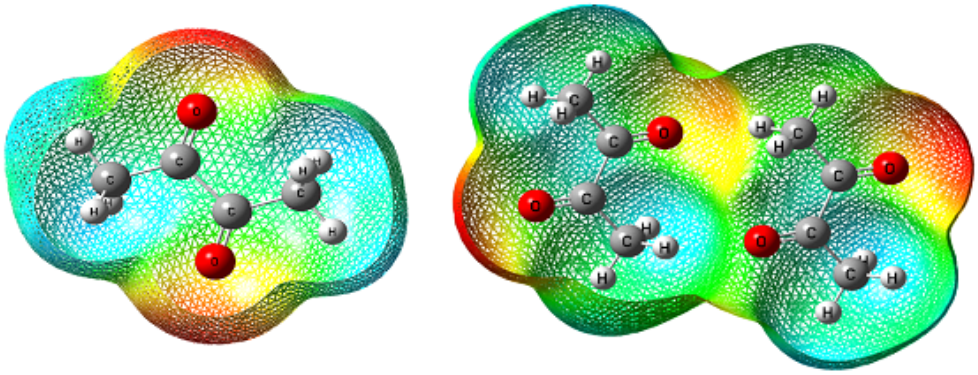


Figure 5. Charge density distribution for DA monomer and dimer. Here: red - oxygen, gray - carbon, white - hydrogen.

It can be seen that in the Raman spectra, the DA+$(H_2O)_5$ cluster has the same cluster appears as DA+$(H_2O)_1$ with the C=O stretching vibration band shift to the low frequency side by ~19 cm^{-1} and the intensity of the band have increased.

Figure 5 shows a visual representation of the charge distribution, the red part has a larger value of the electron density and is more negatively charged. The green part in contrast is that the electron density has reached a minimum and is more positively charged. Also, from a chemical point of view, the red part is the part that is most likely to start the reaction. The simulation shows that a dimer compound can be formed when an intermolecular hydrogen bond is formed between two DA molecules. Dimer formation results in redistribution of charges and a small changein bond lengths, and this is different for proton donor and proton acceptor molecules. The distribution of charges and the change in bond length indicate the structure of the dimer. As the number of hydrogen bond increases, it leads to a significant redistribution of charges in the DA aggregates.

Figure 6 shows a 3D graph of the energy dependence of the angle (between O_{12}-C_6-C_5) and the distance (between C_6=O_{12}) for the DA molecule monomer. The calculations show that the distance between the atoms (0.9 to 1.4 Å) and the energy dependence around the angle (80 to 2000) of the molecule being optimized, respectively. As can be seen from the very bottom of the graph, the optimized energy appears to correspond to certain intervals rather than the exact discrete value of distance and angle.

©Academy of Sciences of Republic of Uzbekistan, 2022

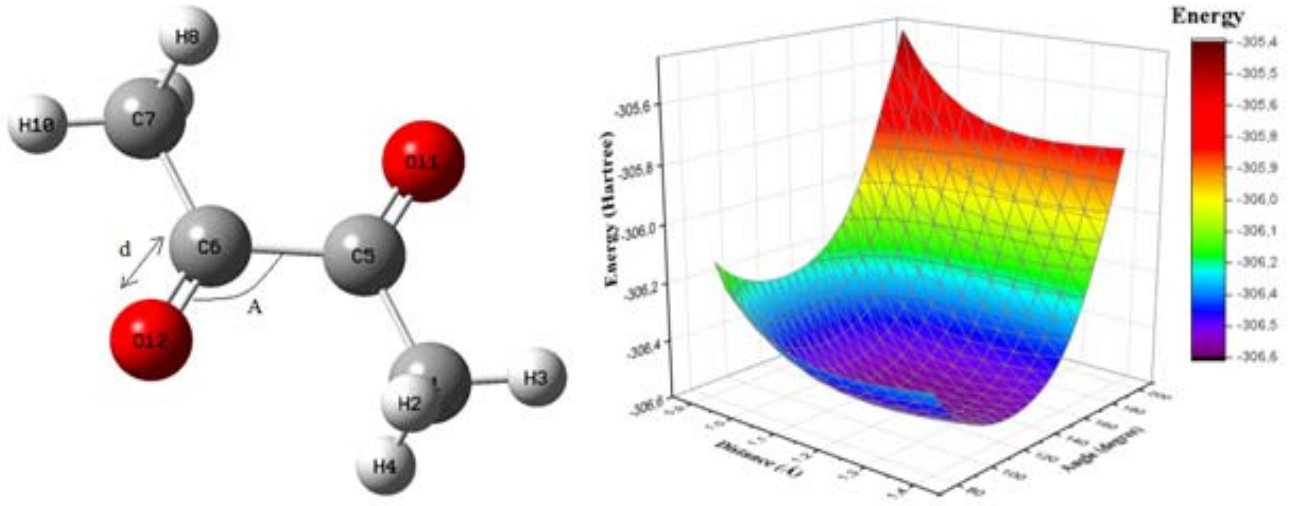


Figure 6. 3D potential energy surface graph for DA monomer. Here atoms of different colors are denoted as follows: red - oxygen, gray - carbon and white - hydrogen.

III. Conclusion

In the experiment, the Raman spectra of DA obtained in the region of 500–2000 cm^{-1} are complex, and several vibrations correspond to several bands with different depolarization ratios. The spectral representation of DA's molecular clusters with isolated monomer, dimer, and water molecules was studied at the B3LYP/DFT approximation.

Experimental and theoretical calculations have shown that the results of DA in the region of 500-2000 cm^{-1} are consistent with a difference of ±2%.

With the increase in the number of molecules in the formation of molecular clusters with the DA water molecule, the saturation of the intermolecular interaction energy corresponding to a single H-bond is observed. This corresponds to DA+$(H_2O)_3$ molecular clusters and this cluster is more stable relative to the others.

Calculations have shown that in the formation of molecular clusters with a DA dimer and a water molecule, the vibration bands shift towards a lower frequency side.

References

[1] D. Dargent, B. Madebene, P. Soulard, B. Tremblay, E.L. Zins, M.E. Alikhani, P. Asselin. J. Phys. Chem. A **121**, 88-97 (2017). https://doi.org/10.1021/acs.jpca.6b10492.

[2] H. Hushvaktov, A. Jumabaev, I. Doroshenko, A. Absanov, Vibrational Spectroscopy **117**, 103315 (2021). https://doi.org/10.1016/j.vibspec.2021.103315.

[3] H. Hushvaktov, A. Jumabaev, G. Murodov, A. Absanov, G. Sharifov. Ukr. J. Phys. **65**, 4 (2020). https://doi.org/10.15407/ujpe65.4.298.

[4] M. Baldwin. A Spectroscopic and Computational Study of Diacetyl and Water Clusters (2021). https://egrove.olemiss.edu/hon_thesis/1657

[5] T. Luisa, M. Profeta, L.S. Robert, J.J. Timothy, D. Stephen, J. Williams. Phys. Chem. A **115**, 9886–9900 (2011). https://doi.org/10.1021/jp204532x.

[6] Sh.J. Takayuki. Agric. Food Chem. **62**, 4048-4053 (2014). https://doi.org/10.1021/jf500615u.

[7] M.J. Mathews, L.W. Scott, W.S. Rodney, P.B. Jason, J. Daniel. Agric. Food Chem. **58** 12761-12768 (2010). https://doi.org/10.1021/jf103251w.

[8] A.G. Zavaglia, R. Fausto. Journal of Mol. Struc. **661-662**, 195–208 (2003). https://doi.org/10.1016/j.molstruc.2003.06.003.

[9] S. Kamei, K. Okuyama, H. Abe, N. Mikami, M. Ito. J. Phys. Chem. **90**, 93-100 (1986). https://doi.org/10.1021/j100273a022

[10] C.B. Johnson, R.T. Holman. Lipids **1**, 371-380 (1966). https://doi.org/10.1007/BF02532539.

[11] L.B. Favero, W. Caminati. J. Phys. Chem. A **113**, 14308–14311 (2009). https://doi.org/10.1021/jp903022x.

[12] Hubbs, F. Ann.. Toxicologic Pathology **36**, 330-344 (2008). https://doiorg.umiss.idm.oclc.org/10.1177/0192623307312694

[13] P. Harber. Toxicological Reviews **25,** 261-272 (2006). https://doi.org/10.2165/00139709-200625040-00006.

©Academy of Sciences of Republic of Uzbekistan, 2022

[14] R. Kanwal. Journal of Occupational and Environmental Medicine **48**, 2, 149-157 (2006). https://doi.org/10.1097/01.jom.0000194152.48728.fb
[15] P. Li, Y. Gao, C. Wang, C. Zhang, X. Guo, D. Xiao. J. Agric. Food Chem. **66**, 32, 8556-8565 (2018). https://doi.org/10.1021/acs.jafc.8b02356.
[16] S.S. More, A. Raza, R. Vince. J. Agric. Food Chem. **60**, 3311-3317 (2012). https://doi.org/10.1021/jf300180e.
[17] A.J. Poulose, P.E. Kolattukudy. Int. J. Biochem. **18**, 9, 807-812 (1986). https://doi.org/10.1016/0020-711x(86)90057-1.
[18] M.J. Frisch, G.W. Trucks, H.B. Schlegel, G.E. Scuseria, M.A. Robb, J.R. Cheeseman, G. Scalmani, V. Barone, B. Mennucci, G.A. Petersson, H. Nakatsuji, M. Caricato, X. Li, H.P. Hratchian, A.F. Izmaylov, J. Bloino, G. Zheng, J.L. Sonnenberg, M. Hada, M. Ehara, K. Toy-ota, R. Fukuda, J. Hasegawa, M. Ishida, T. Nakajima,Y. Honda, O. Kitao, H. Nakai, T. Vreven, J.A. Montgomery, jr., J.E. Peralta, F. Ogliaro, M. Bearpark,J.J. Heyd, E. Brothers, K.N. Kudin, V.N. Staroverov, R. Kobayashi, J. Normand, K. Raghavachari, A. Rendell, J.C. Burant, S.S. Iyengar, J. Tomasi, M. Cossi, N. Rega, J.M. Millam, M. Klene, J.E. Knox, J.B. Cross, V. Bakken, C. Adamo, J. Jaramillo, R. Gomperts, R.E. Stratmann, O. Yazyev, A.J. Austin, R. Cammi, C. Pomelli, J.W. Ochterski, R.L. Martin, K. Morokuma, V.G. Za-krzewski, G.A. Voth, P. Salvador, J.J. Dannenberg, S. Dap-prich, A.D. Daniels, O. Farkas, J.B. Foresman, J.V. Ortiz, J. Cioslowski, D.J. Fox. Revision A.02. Gaussian 09 (Gaussian, Inc., Wallingford CT, 2010).
[19] N. Klaus, R.J. Norman. Wiley Online Library **64**, 5, 707-713 (1960). https://doi.org/10.1002/bbpc.196000031.

Диацетил-сув кластерларини комбинацион сочилиш ва назарий ҳисоблашлар ёрдамида ўрганиш

А. Жумабаев, Ҳ. Хушвақтов, А. Абсанов, А. Норқулов, Б. Илтизаров

Самарқанд давлат университети, Университет хиёбони 15, 140104, Самарқанд, Ўзбекистон

Ушбу ишда диацетил ва сув молекулаларида молекулалараро ўзаро таъсирларни тебраниш спектрида намоён бўлиши ўрганилди. 500–2000 $см^{-1}$ оралиқда олинган комбинацион сочилиш спектрлари таҳлил қилинди ва назарий ҳисоблаш натижалари билан таққосланди. Шунингдек, ишда диацетил молекулалари учун симулация ёрдамида биринчи марта заряд зичлик тақсимоти ва 3D потенциал энергия графиклари ўрганилди. ДА сув молекуласи билан молекуляр кластерлар ҳосил бўлишида молекулалар сони ортиши билан битта H-боғланишга тегишли молекулалараро таъсир энергияси тўйиниши кузатилади ва бу ДА+$(H_2O)_3$ молекуляр кластерларига тўғри келиб, бу кластер бошқаларига нисбатан барқарор деган хулосани беради.

Калит сўзлар: диацетил, сув, DFT ҳисоблашлар, комбинацион сочилиш спектри, водород боғланиш, симулация.

©Academy of Sciences of Republic of Uzbekistan, 2022